

# A comparative study of laser surface hardening of AISI 410 and 420 martensitic stainless steels by using diode laser

Moradi, M., Arabi, H., Jamshidi Nasab, S. & Benyounis, K. Y.

Author post-print (accepted) deposited by Coventry University's Repository

**Original citation & hyperlink:**

Moradi, M, Arabi, H, Jamshidi Nasab, S & Benyounis, KY 2019, 'A comparative study of laser surface hardening of AISI 410 and 420 martensitic stainless steels by using diode laser', Optics and Laser Technology, vol. 111, pp. 347-357.

<https://dx.doi.org/10.1016/j.optlastec.2018.10.013>

DOI 10.1016/j.optlastec.2018.10.013

ISSN 0030-3992

Publisher: Elsevier

**NOTICE: this is the author's version of a work that was accepted for publication in Optics and Laser Technology. Changes resulting from the publishing process, such as peer review, editing, corrections, structural formatting, and other quality control mechanisms may not be reflected in this document. Changes may have been made to this work since it was submitted for publication. A definitive version was subsequently published in Optics and Laser Technology, 111, (2019) DOI: 10.1016/j.optlastec.2018.10.013**

© 2019, Elsevier. Licensed under the Creative Commons Attribution-NonCommercial-NoDerivatives 4.0 International <http://creativecommons.org/licenses/by-nc-nd/4.0/>

Copyright © and Moral Rights are retained by the author(s) and/ or other copyright owners. A copy can be downloaded for personal non-commercial research or study, without prior permission or charge. This item cannot be reproduced or quoted extensively from without first obtaining permission in writing from the copyright holder(s). The content must not be changed in any way or sold commercially in any format or medium without the formal permission of the copyright holders.

This document is the author's post-print version, incorporating any revisions agreed during the peer-review process. Some differences between the published version and this version may remain and you are advised to consult the published version if you wish to cite from it.

# **A Comparative Study of Laser Surface Hardening of AISI 410 and 420 martensitic stainless steels by using diode laser**

Mahmoud Moradi<sup>1,2,\*</sup>, Hossein Arabi<sup>1,2</sup>, Saied Jamshidi Nasab<sup>1,2</sup>, Khaled Y. Benyounis<sup>3</sup>

1-Department of Mechanical Engineering, Faculty of Engineering, Malayer University, Malayer, Iran

2-Laser Materials Processing Research Center, Malayer University, Malayer, Iran

3- School of Mech. & Maun. Eng., Dublin City University, Dublin, Ireland

## **Abstract:**

Laser surface hardening process is one of the new technologies for improving the surface of metals, especially steels, which in recent decades has received a lot of attention. This paper surveys the capability of laser surface hardening of AISI 410 and AISI 420 martensitic stainless steel by using continues wave diode laser with a maximum power of 1600 W, experimentally. Microstructure of the laser treated area by using optical microscope (OM), Field emission Scanning Electron Microscope (FESEM), and XRD were investigated and compared. Geometrical dimension, micro-hardness deviation (MHD) from the micro-hardness of the base metal, ferrite percentage, and the grain size of the hardened zone are the other considered responses. The results indicate that in the same input parameters the AISI 420 has higher surface hardness and less penetration depth and width than the AISI 410 stainless steel. Observations showed that a laser surface hardened layer of AISI 410 is about 620 HV with 1.8 mm depth and while for AISI 410 is about 720 HV with 1.2 mm depth is obtained. Comparing the results with the furnace hardening heat treatment show that the laser hardening process is more effective and precise than conventional processes.

## **Key words:**

Laser Surface Hardening; AISI 410; AISI 420; Microstructure; Micro-hardness.

## **1-Introduction**

Laser is a heat source that increases the energy heat input of the metal surface, while the bulk material (metal volume) act as heat transfer at high cooling rates [1]. Surface hardening is used to improve the Tribological properties (corrosion, erosion, hardness...) of a material [2]. Among various laser surface treatments, laser transformation hardening (LTH) is one of the most useful and the simplest and precise methods. Because it does not require any accessories. Laser processing is used for numerous industrial applications such as laser

welding and brazing [3-9], laser hardening [10-14], laser drilling [15], laser cutting [16-17] and laser forming [18-22]. Diode laser is one of common laser types in industry. This type of laser with high accuracy heat treats the surface of matter. Although power densities are still lower for HPDL than CO<sub>2</sub> and Nd: YAG laser, many applications can benefit from HPDL [23]. Figure 1 illustrates a schematic of the laser surface hardening process in which the focal plane position is shown.

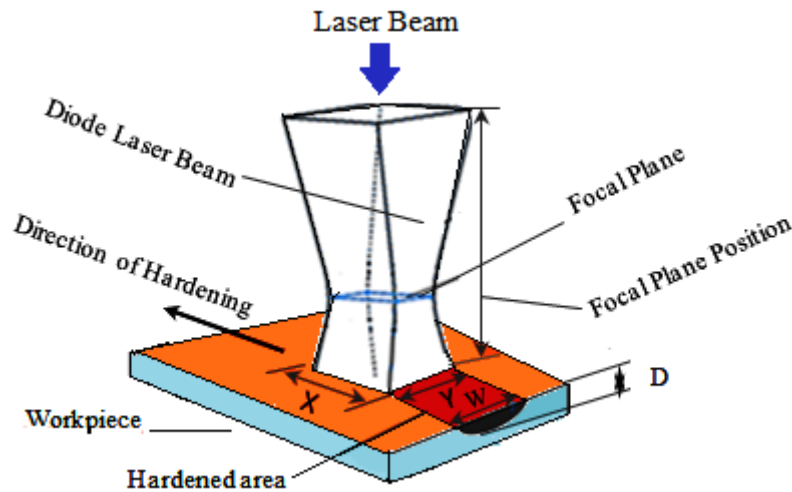


Fig. 1 schematic of the laser surface hardening process [24].

So many researches done on martensitic stainless steel to develop the material properties [25-28]. Mahmoudi et al. [29] carried out surface hardening of AISI 420 martensitic stainless steel by means of pulsed Nd:YAG laser, which in their research hardness in depth of hardened layer and width of this layer were investigated, also overlap of laser hardened lines and corrosion resistance of this steel after laser treatment were evaluated. Francisco Cordovilla et.al [30] by simulating laser hardening process and comparing the results of simulation with experimental data of laser hardening of AISI 4140 low alloy steel, investigated the effect of laser lines overlap. Wear and corrosion resistance of AISI H13 tools steel which hardened up to 800 Vickers was studied by Telasang et.al [31]. Goia et al. [32] in 2010 conducted an investigation using a high-power 2 kW fiber laser on AISI D6 steel with laser hardening and then the effect of melting created by different laser powers in the structure was investigated. In their study by adjusting the focal point position of 40 mm, the laser power of 500 watts and the scanning speed of 6.5 mm/s and the percentage of overlapping of 80%, hardness of melted area between 400 and 500 Vickers; the heat affected zone was 800 Vickers; and hardness depth was 1.8 mm. Zirepour et al. [33] in 2014 evaluated the electro-chemical corrosion behavior of AISI 420 stainless steel after laser surface

hardening. The AISI 420 martensitic stainless steel is achieved by this laser with a maximum hardness of 700 Vickers. As a result, the corrosion resistance of the AISI 420 martensitic stainless steel was increased by laser hardening compared to the metal substrate and its corrosion potential reached 113 mili-volts. Benyounis et al. [34] in 2016, in a study on the coating of nitrogen gas on the 316L, 316, and 304 metals were carried out according to design of experiments method. Their results show that 316L stainless steel has a surface hardening better than 316 and 304 metals at temperatures above 450 ° C. The surface hardness of 316L by gas nitrogen method is about 5 times than the base metal. The response surface method is an effective method for studying nitrogen gas, which lowers the number of experiments and saves time and cost. Moradi et al. [35] in 2017, in a study performed the laser surface hardening of AISI 410 martensitic stainless steel with a maximum power of 700 watts by Nd: YAG laser. The focal point position and laser pulse energy are the laser parameters in this study. The results showed that due to the solid state transformation and dissolution of carbides in the martensitic field in the laser surface hardening, improvement in surface hardening was obtained. The highest depth of the hardened layer was 350 microns and the maximum hardness was 747 Vickers.

In the present study, the laser surface hardening in the same input parameters was investigated using high power diode laser on AISI 410 and AISI 420 stainless steel. Surface hardness, geometrical dimensions of the hardened area (depth, width and angle), as well as the micro-hardness changes in depth and width were measured and analyzed. Micro-hardness deviation (MHD) from the base metal micro-hardness is another parameters that is investigated. Microstructure of hardened areas was analyzed by Optical microscopy and Field emission scanning electron microscope (FESEM). The results showed that the AISI 420 stainless steel has higher surface hardness and less penetration depth and width than the AISI 410 stainless steel. Also in the microstructure of AISI 410, the ferrite content in martensitic field is more than the microstructure of AISI 420, and also the AISI 420 has a more uniform structure, (a little ferrite and carbide in the martensitic field).

## **2-EXPERIMENTAL WORK**

AISI 410 and AISI 420 martensitic stainless steels were used in this study as materials work piece. Chemical compositions of the two materials are listed in [Table 1](#). The chemical composition measured by quantimeter in laboratory conditions at 28°C and humidity of 14 percent according to the ASTM E1019 standard. Sample preparation operations and micro-

structure study was done. The samples with a thickness of 10 mm were prepared of 65 mm diameter rod by machining and the sample surface was grounded.

Table .1 Chemical composition of AISI 410and AISI 420 stainless steels (Wt. %)

| Steel name | C    | Si   | Ni   | Mn   | P     | S     | Cu   | Cr    | Mo   | Al    | Fe      |
|------------|------|------|------|------|-------|-------|------|-------|------|-------|---------|
| AISI 420   | 0.2  | 0.5  | 0.08 | 0.51 | 0.034 | 0.005 | 0.02 | 12.49 | 0.01 | 0.002 | Balance |
| AISI 410   | 0.15 | 0.28 | 0.12 | 0.51 | 0.018 | 0.024 | 0.11 | 13.5  | 0.03 | 0.008 | Balance |

In order to the surface hardening of the steels, in this study, the diode laser with a maximum power of 1600 watts was used. The ranges of experimental settings, the laser power, scanning speed and the focal point position parameters was considered 1200-1600 watts, 5-6 mm/s, and 60-70 mm, respectively. Table 2 illustrates the settings and results of laser surface hardening of AISI 410 and AISI 420 steels. Figure 2 shows the image of diode laser surface hardening of AISI 410 and AISI 420.



Fig. 2 Images of Laser Surface Hardening by diode laser a) AISI 410 b) AISI 420

Figure 3 illustrates the diode laser device in the present study, which is performing laser surface hardening process on the AISI 410 and AISI 420 stainless steels.



Fig. 3 The image of the diode laser device used in this study

Table. 2 Settings and results of laser surface hardening of AISI 410 (A1-A2-A3) - AISI 420 (B1-B2-B1)

| Sample number | Input parameters      |                           |                 | Output results         |                        |                        |              |              |                        |
|---------------|-----------------------|---------------------------|-----------------|------------------------|------------------------|------------------------|--------------|--------------|------------------------|
|               | Scanning speed (mm/s) | Focal plane position (mm) | Laser Power (w) | Maximum Hardness (h v) | Depth of Hardness (mm) | Width of Hardness (mm) | MHD in depth | MHD in width | Ferrite percentage (%) |
| A1            | 6                     | 70                        | 1600            | 620                    | 1.82                   | 8.31                   | 18813.70     | 28651.61     | 0.51                   |
| B1            | 6                     | 70                        | 1600            | 800                    | 1.32                   | 6.07                   | 42023.25     | 63001.46     | 0.08                   |
| A2            | 5                     | 65                        | 1400            | 600                    | 2.20                   | 8.13                   | 18658.42     | 26621.62     | 0.65                   |
| B2            | 5                     | 65                        | 1400            | 720                    | 1.25                   | 6.12                   | 39782.01     | 52012.23     | 0.12                   |
| A3            | 6                     | 60                        | 1200            | 520                    | 2.01                   | 8.10                   | 15090.53     | 20074.58     | 1.52                   |
| B3            | 6                     | 60                        | 1200            | 710                    | 1.04                   | 6.24                   | 35014.30     | 50079.92     | 0.24                   |

The beam incident on the sample surface is rectangular in cross section and increasing the focus-material distance increases the beam size in both the direction of travel (x) and perpendicular to that direction (y). The FPP = 60 mm means that the focal plane is exactly positioned on the material surface. The dimensions of the beam for each focal plane position used here are given in Table 3. Each hardened sample after laser hardening process at the middle of the hardened track was sectioned. Phenolic thermosetting resin was used for mounting the laser hardened cut specimens. Metallography samples prepared according to the ASTM E3-11 standard guide for preparation of metallographic specimens by conventionally grinding, polishing and etching in the villa's reagent (C6H3N3O7 2gr, Hcl 5cc, C2H5OH 100cc). Optical microscopy (OM) and field emission scanning electron microscopy (FESEM) were used to investigate the microstructure of the hardened zone. The geometry features of the hardened area (width and depth), see Figure 5, were captured using BUEHLER MET B7 optical microscope and by the ImageJ software the geometrical dimensions were precisely measured. Micro hardness measurements were carried out by a micro-indentation tester (BUEHLER, USA) along a line 50  $\mu$ m below the surface of the cross-section of the hardened zone by using of ASTM E384 standard. Figure 4 shows the optical microscopy and micro hardness devices used in the present study.

Table . 3 The relationship between the Incident Beam Length, Width and Area.

| Focal Plane Position | Incident Beam Length (x) | Incident Beam Width (y) | Incident Beam Area (x-y) |
|----------------------|--------------------------|-------------------------|--------------------------|
| 60 mm                | 1.50 mm                  | 8.00 mm                 | 12.00 mm <sup>2</sup>    |
| 65 mm                | 2.55 mm                  | 9.94 mm                 | 25.34 mm <sup>2</sup>    |
| 70 mm                | 3.60 mm                  | 11.88 mm                | 42.77 mm <sup>2</sup>    |



**Fig. 4** The image of the optical microscopy (a), and Micro hardness device (b) used in this study

The percentage of ferrite phase at the middle of the structure of the hardened layer was measured by Celemex software. The micro hardness measured by using a maximum load of 100 gr and a dwell time of 30 s. The profiles of the hardness were plotted for each sample along the line from the center of the hardened area toward the base metal in depth (from the surface up to the penetration depth) and width directions of the hardened zone. Figure 6 depicts the cross-sectional view of Vickers indenters in surface and depth of hardened layer. Micro hardness deviation (MHD) from the base metal micro hardness was determined by Equation 1:

$$MHD = \sum_{i=1}^n (x_i - x_{bm}) / n \quad (1)$$

where  $x_i$  is microhardness of point  $i$  and  $x_{bm}$  is base metal microhardness,  $n$  is the number of measured microhardness points. In this paper,  $n$  is 10 and  $x_{bm}$  equal 330 Vickers for AISI 410 and 210 for AISI 420.

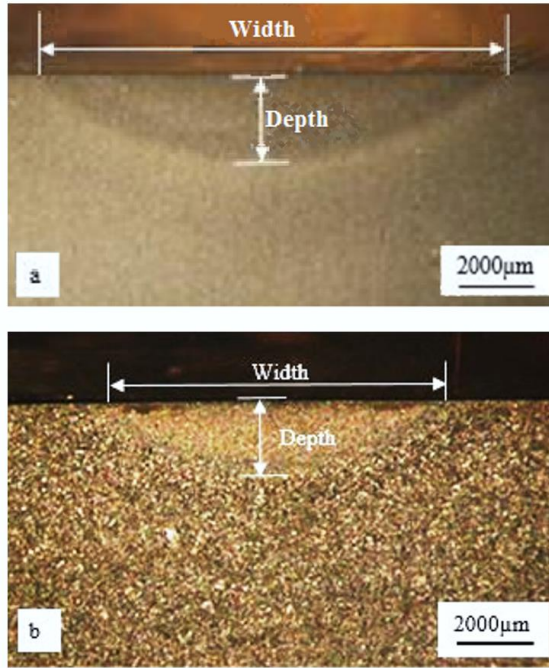


**Fig.5** Geometrical dimensions of laser hardened samples cross section,(a) AISI 410,(b) AISI 420

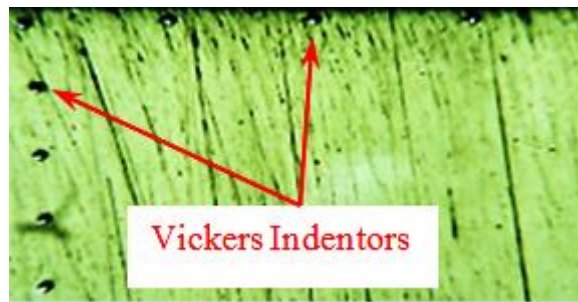
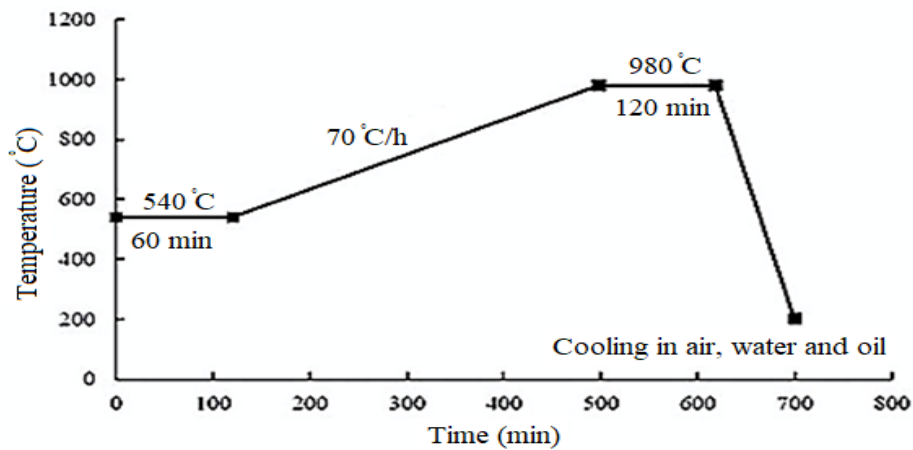


**Fig. 6** Image of Vickers indentors in depth and width of hardened area

For comparing the laser surface hardening method with conventional method, the furnace heat treatment according to ASTM A217/A217M-14 standard presented in [Figure 7](#) was conducted. The material preheated to 540 °C for 600 minutes and heated to 980 °C with the rate of 70 °C/hour and was kept for 120 minutes. The samples quenched in oil, water and air.



### 3-Results and discussion

In this paper, the effect of diode laser surface hardening with the same input parameters on AISI 410 and AISI 420 stainless steel has been investigated. In order to study the surface properties, the geometrical dimensions of the hardened area (depth and width), the micro hardness distribution in depth and width, Micro hardness deviation from base material (MHD) in depth and width of the hardened area obtained and the micro-structure of the hardened area were analyzed.

#### 3-1 Micro hardness distribution of hardened area

Figure 8 shows the profile of micro hardness distribution from the surface of the sample to depth in laser surface hardening of AISI 410 stainless steel.

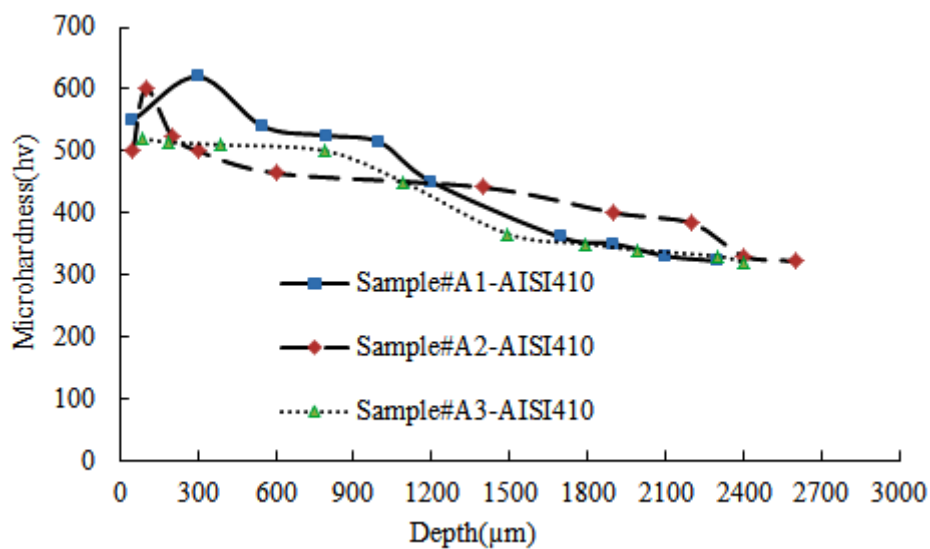


Fig. 8 Micro hardness in the depth of hardened layer of AISI 410

It is well visible in Figure 8 that the surface hardness increases due to laser surface treatment. By moving away from the surface to the base metal, the hardness gradually decreases until it reaches the hardness of the base metal.

The micro-hardness distribution could be explained by heat input of the laser energy to the material. The heat input presented in Equation 2 is used for better understanding of the process and explaining this phenomenon.

$$\text{Heat input} = \text{Laser power} / \text{Scanning Speed} \quad (2)$$

Thus heat input increases when the laser power increases and the scanning speed decreases. By reducing the scanning speed the interaction time of the laser and material will be enhanced. Then more part of the surface of the material will be heated and the depth of hardened layer increases. Increases in the heat input lead to increases the hardness, while for A1 and A3 the heat input are 266.6 (j/mm) and 200 (j/mm), respectively.

In the hardened area, fine-grained martensitic and ferrite phase are dispersed. Due to the high speed of the high cooling mechanism and the lack of sufficient time to dissolve ferrite particles, dissolution of the incomplete ferrite is performed and remains in the hardened structure. This has brought down the hardness in these areas [37]. Figure 9 shows the profile of micro hardness distribution from the surface to depth in laser surface hardening of AISI 420 stainless steel.

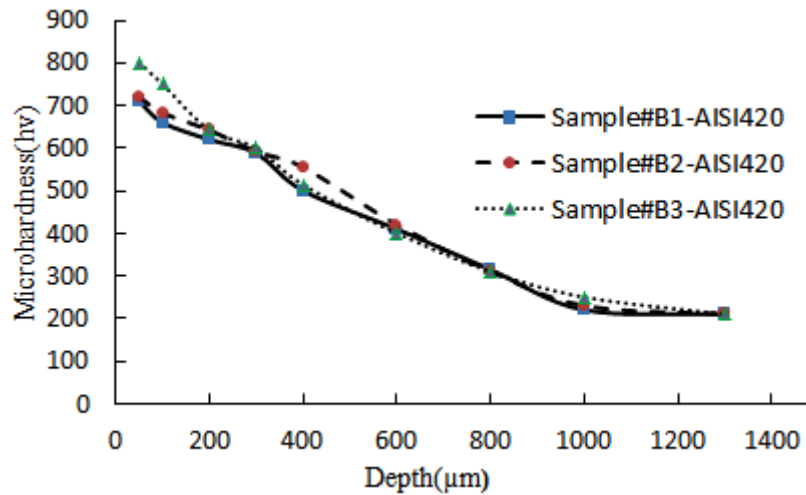


Fig. 9 Micro hardness in the depth of hardened layer of AISI 420

As shown in Figures 9 and 10, AISI 420 has a higher hardness than AISI 410. The reason for this increase is related to hardenability of the AISI420 than the AISI410.

The perlite transformation is a phenomenon effect on the laser hardening process. In general, any factor that transmits perlite formation lines to the right in the CCT diagram provides the possibility of martensite formation in lower cooling tracks. Therefore, the transfer of the nose of the CCT diagram to the right is accompanied by an increase in hardness. In other words, it can be said that any factor that reduces the germination rate and the perlite growth (increases the time needed for germination and the growth of perlite) increases the hardenability in the steels [38]. These factors are: austenite grains size, carbon percentage, alloy elements, non-metallic impurities and impurities, homogeneity of the microstructure. Due to the higher carbon content, the more homogeneous structure, and the finer grain size of AISI 420 than the AISI 410, the hardenability of AISI 420 is higher than AISI 410.

### 3-2 Micro hardness deviation from base material (MHD)

Micro hardness deviation from base material (MHD) is explained in section 2, experimental work. The MHD in depth and width is one of the important aspects of the output responses in this research. In fact this parameter indicates the uniformity of hardness in the hardened zone

[39-40]. If the hardness decreases gradually from surface to depth, the hardness profile decreases slightly and the MHD in depth will be increased. Higher MHD in the laser hardening is more desirable. Considering that the hardness from surface to the depth in the center of the hardened zone is reduced uniformly, by increasing hardness the MHD also increases. Therefore it could be said that the MHD has a direct relationship with hardness. Figure 10 depicts the variation of MHD via Micro hardness variations of AISI 420 & AISI 410.

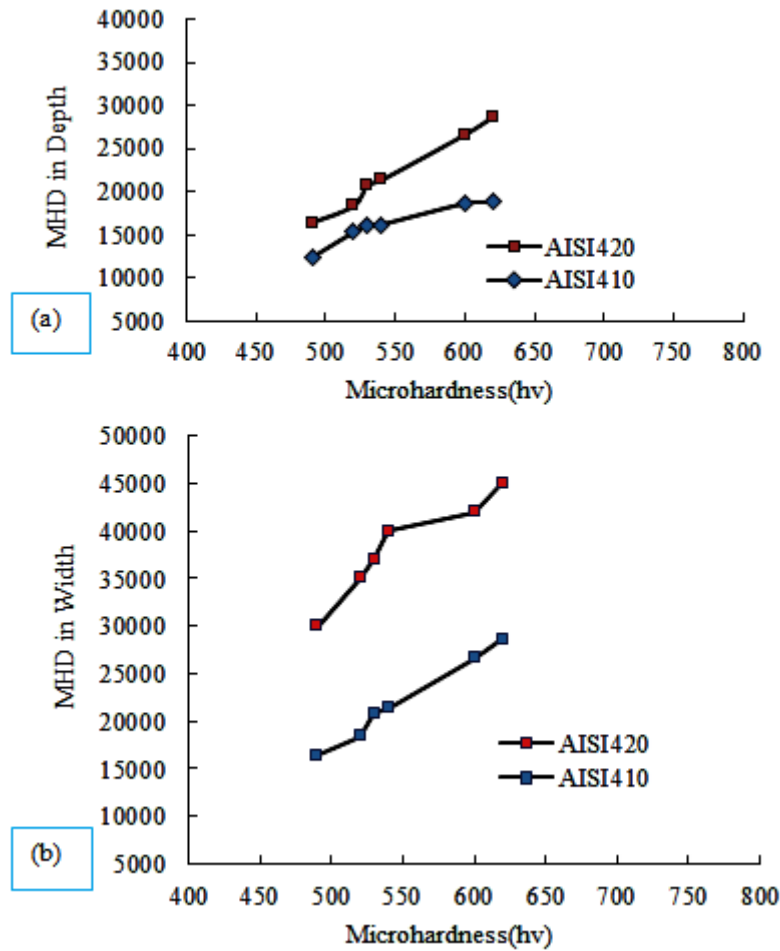


**Fig. 10** MHD profile of AISI 420 & AISI 410 in Micro hardness hardened area, **a)** Depth, **b)** Width. As shown in Figure 10, due to the higher hardness of AISI 420 stainless steel, the MHD in depth and width of the hardened area of AISI 420 is more than the AISI 410 stainless steel. The maximum hardness in the AISI 410 and AISI 420 laser hardened samples are 620 Hv and 720 Hv, respectively. Thus, the AISI 410 stainless steel hardness increased by 88% and the hardness of AISI 420 stainless steel increased by 227%. These percentages also show the higher hardenability of AISI 420.

### 3-3 Geometrical dimensions of hardened layer

Considering the geometrical dimension presented in Table 2 it seen that the depth of hardness in samples#3 are larger that samples#1. This trend could be explained by energy beam density shown in Equation 3:

$$\text{Beam density} = \text{Laser power} / \text{Incident beam area} \quad (3)$$

By increasing the energy beam density the temperature influenced on the sample surface increases. Therefore the austenitic temperature rises so the hardness and the depth of the hardened area are increased. The incident beam area is mentioned in Table 3. So the beam density calculated by Equation 3 and for samples#3 and samples#1 are  $100 \text{ W/mm}^2$  and  $37.41 \text{ W/mm}^2$ , respectively. So having more beam density lead to increases in the depth and the geometry of the hardened layer.

Figure 11 shows the schematic of the diode laser beam distribution. As regards laser beam energy is used as a plane distribution (rectangular), the higher temperature in the center of the laser beam than in the corners of the beam. Therefore, there is a higher temperature in the center of the beam and with move away from the center; the energy intensity of the laser beam drops [41].

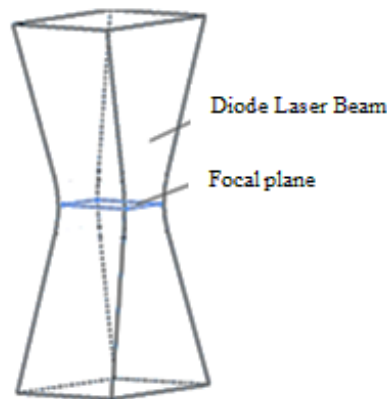
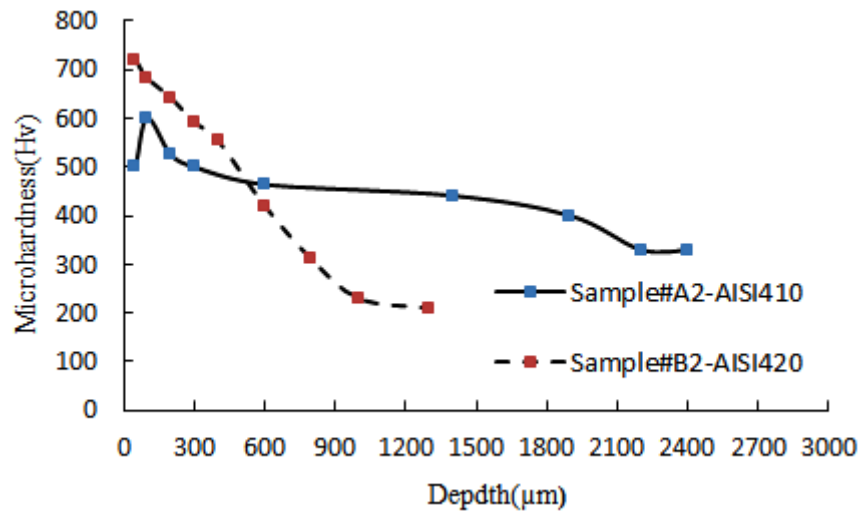


Fig. 11 Schematic of diode laser beam distribution

Figure 12 shows a comparison of the micro-hardness distribution at the depth of the AISI 410 and AISI 420 stainless steels. From Figure 12, we conclude that according to the same input parameters of a diode laser, the depth of penetration of the hardened area in AISI 410 is more than the AISI 420. The depth of laser penetration is expressed in terms of the absorption of laser energy.



**Fig.12** Comparison of the micro-hardness distributions the laser hardened depth of AISI 410# **A2** and AISI 420 # **B2**

The laser absorbed energy is dependent on the following parameters [42]:

- 1- Optical constants of the surface of the metal: includes surface absorption coefficient and surface reflection coefficient.
- 2- Physical characteristics of the laser: include wavelength, polarization, and laser power density.
- 3- The percentage of alloys in the chemical composition of steel.
- 4- Physical properties of steel: including density and thermal conductivity of steel.
- 5- Surface topography: includes polished or uneven surface.
- 6- Metallurgical factors of steel structure: include grain size, structural particle shape and metallography conditions.

Given that the specifications of the diode laser are used and the surface topography conditions for two steel is the same. Therefore, only the parameters 3, 4, and 6 of the above mentioned are considered. In general, by increasing the composition of the alloying elements, the velocity of the thermal conductivity in the steel increases. [Table 4](#) shows the comparison of the physical parameters of the AISI 410 and AISI 4120 steels.

Table. 4 Comparison of physical properties of AISI 410 and AISI 420 [42]

| Physical properties | Density, lbs/in <sup>3</sup> (g/cm <sup>3</sup> ) | Thermal Conductivity, BTU/hr/ft/(W/m/k) | Electrical Resistivity, μΩ.in. (μΩ.cm) | Coefficient of Thermal Expansion, in/in °F (μm/m/k) | Modulus of Elasticity, ksi. (Mpa) | Specific Heat, BTU/lbs.°F(kj/kg/k) |
|---------------------|---|---|--|---|-----------------------------------|------------------------------------|
| AISI 410            | 7.74  | 24.9                                    | 55                                     | 10.2  | 200                               | 0.46                               |
| AISI 420            | 7.8   | 24.9                                    | 57                                     | 9.9   | 200                               | 0.46                               |

According to [Table 4](#) the thermal conductivity of AISI 410 and AISI 420 is similar. But due to the change in the alloying elements in the steel, the composition of the alloying elements in these two steels will change. With a significant increase in alloying elements, the thermal conductivity increases. In this research the percentage of alloying elements in AISI 410 (%14.75) is higher than AISI 420 (%13.851), see [Table 1](#). Therefore, the velocity of the thermal conductivity and also the thermal energy penetration in AISI 410 are higher than of the AISI 420.

The ASTM-112 standard is used to determine the grain size. Due to the Martensite particles in the structure of the investigated metals are very small, it is not possible to determine their size. Therefore, to determine the grain size according to the ASTM-112 standard, the normalize heat treatment cycle should be initiated at 850 ° C for one hour and then cooled at the furnace temperature. After performing the mentioned heat treatment with a suitable etching solution, the initial austenite grains are investigated. In fact, due to the size of austenite, grain size is evaluated. By using Nital etchant (98 ml ethanol solution and 2 ml nitric acid), the initial austenite grain size, In the AISI 410 and AISI 420 from ASTM Grain Size Number 7 (30μm) and 8 (22 μm) (for the base metal) reach to ASTM Grain Size Number 11 (7μm) and 13 (2 μm), respectively. According to the ASTM-112 standard, we know that by increasing in the ASTM Grain Size Number the grain size becomes smaller. Therefore, AISI 420 has a finer grain size and lower laser penetration depth [\[43\]](#). But the shape of the particles is stretched in the structure of AISI 410. Therefore, the study of the grain size, confirms that the penetration of the laser beam and the penetration depth in AISI 410 is greater than AISI 420.

The relationship between the grain size and mechanical properties is known by the Hall–Petch relation [\[43-44\]](#). [Equation 4](#) expresses the Hall–Petch relation:

$$\sigma_0 = \sigma_i + KD^{-1/2} \quad (4)$$

Where  $\sigma_i$  is yield stress,  $\sigma_0$  is the friction stress, K is the locking parameter and D is the mean diameter of the grain.

By decreasing the size of the grains the value of the grain-boundaries in the structure will increase. The grain boundaries impede dislocation movements. So when the dislocations could not move easily the strength of the material will increase. Grain size has an effective influence on most mechanical properties. For example, at room temperature, hardness, yield strength, tensile strength, fatigue strength and impact strength all increase with decreasing grain size [45-47]. These reasons present that by increasing the hardness by laser hardening technique, not only the grain sizes reduce, but also the strength of the material and mechanical properties improve. If the shape of the particles inside the structure is larger, the rate of heat penetration and thermal conductivity in that structure are increased. Due to the shape of the ferrites that are stretched in the AISI 410 structure and the carbides in the AISI 420 are dense and spherical particles, the heat transfer rate in the AISI 410 is greater than that of the AISI 420. Therefore, the depth of laser penetration and the depth of the laser hardened area in AISI 410 steel is higher than the AISI 420 steel. It is concluded from Figure 13 that the width of the laser hardened in AISI 410 steel with similar input parameters is larger than the AISI 420 steel.

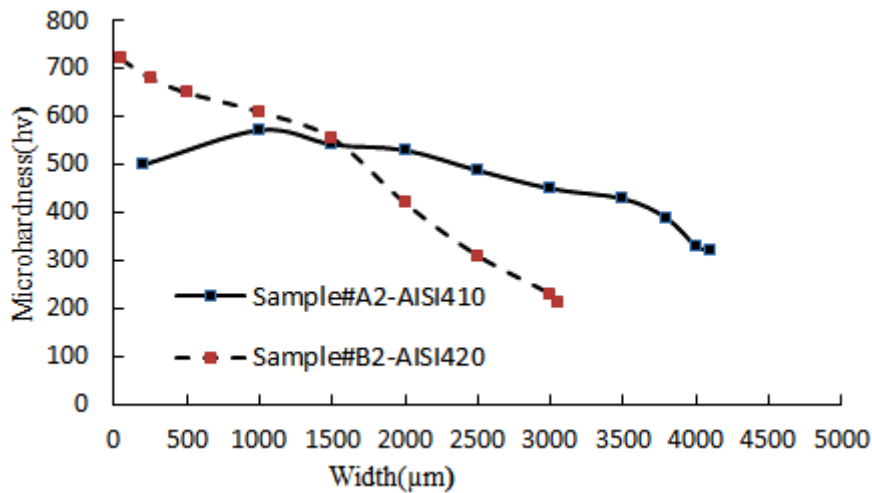


**Fig.13** Comparison of the micro-hardness distribution in the laser hardened width of AISI 410# **A2** and AISI 420 # **B2**

The heat transfer in the width of the hardened area is similar to that described for penetration of the particle in the depth of the hardened area. Therefore, the depth and width of AISI 410 hardened area is larger than the AISI 420.

### **3-4 Microstructure of hardened layer**

In the laser hardening process, there is not enough time to completely dissolve the ferrites and carbides. Controlling the amount of laser heat input energy by increasing the laser power,

decreasing the scanning speed, and reducing the focal plane position can help to dissolve them completely and to create a complete martensitic in the structure. In [Figures 14-a](#) and [14-b](#), the microstructures of raw material of AISI 410 and AISI 420 stainless steel are shown.

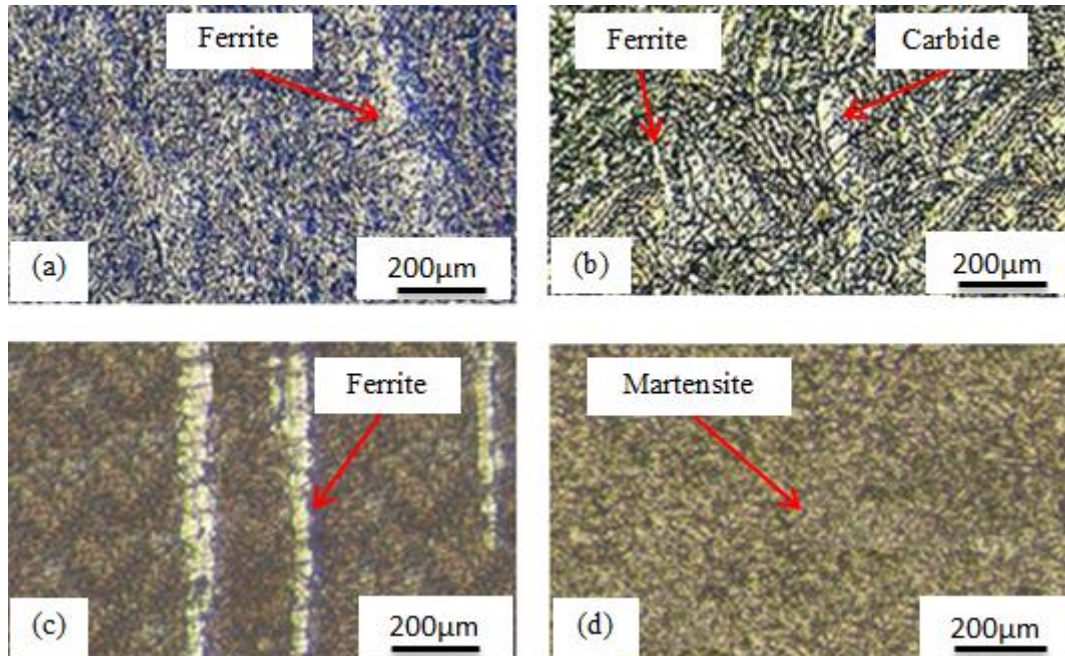


**Fig. 14** Images of microstructure of raw material, AISI 410# **a** and AISI 420# **b**  
Micro structure of hardened samples by diode laser, AISI 410# **c** and AISI 420# **d**

The ferrite phase is formed in the air-cooled stage for quench-temper steels. In the event that after the steel production stage is quenched in the air at high speed or in water-cooled, the ferrite phase does not form. [Figure 14-c](#) shows the microstructure of laser hardening of AISI 410 samples in which there is ferrite phase. In samples with higher laser power, the austenitic temperature is higher for the phase transformation and the austenitic grains become smaller, hence, the percentage of ferrite phase decreases. When we control the time at this temperature, that is to say, reduce the laser scanning speed, the austenite grains become more uniform and the ferrite percent is even lower. So by increasing laser power, the austenitic temperature rises. By decreasing the laser scanning speed, the time factor for uniformity of austenite grains is provided. [Figure 14-d](#) depicts the microstructure of laser hardening of AISI 420 samples in which the carbide particles are fine and dispersed, and the ferrite particles are also smaller. Therefore, a more uniform structure is observed. The microstructure images of AISI 410 and AISI 420 taken with a Field Emission Scanning Electron Microscope (FESEM) are shown in [Figure 15](#).

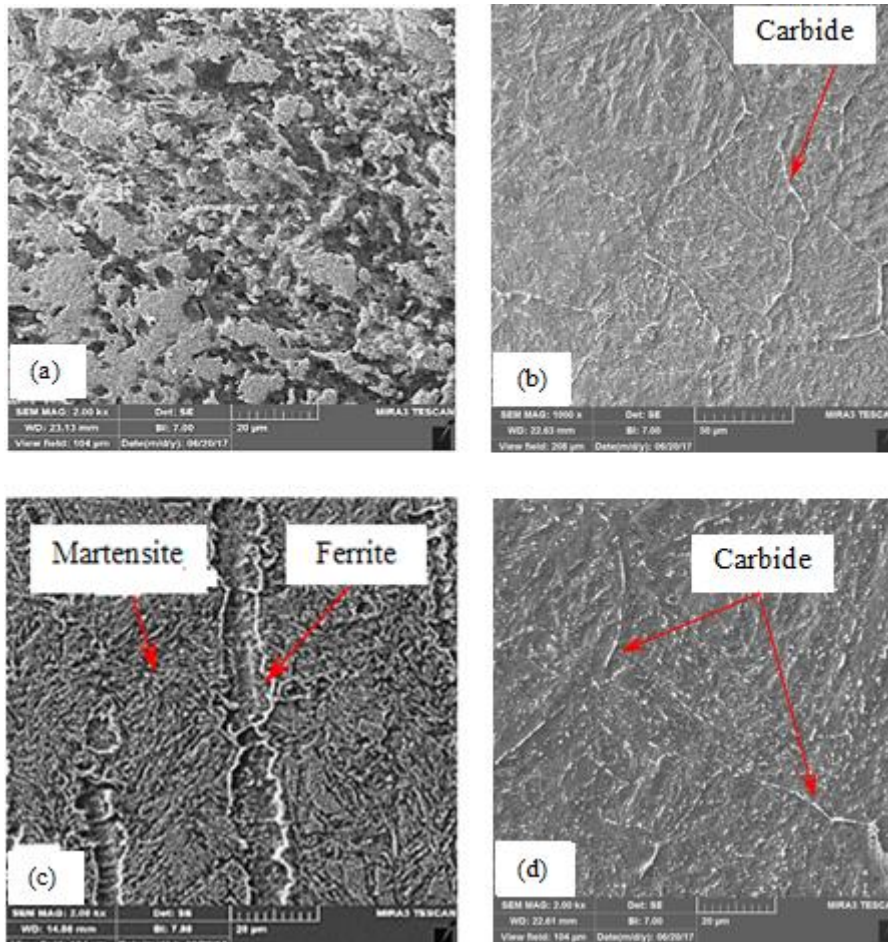


**Fig.15** images of microstructure of raw material by FESEM , AISI 410# **a** and AISI 420 # **b**  
 Micro structure of hardened samples by FESEM, AISI 410#**c** and AISI 420#**d**

The [Figures 15-a](#), [15-b](#), [15-c](#), and [15-d](#) correspond to microstructure of raw material of the AISI 410, raw material of AISI 420, laser hardened of the AISI 410, and laser hardened of AISI 420, respectively. As shown in [Figure 15-a](#), the AISI 410 structure is composed of a ferrite phase in the martensite field. And in [Figure 15-c](#), after laser hardening, ferrite particles are more integrated and more uniform in AISI 410 structure. Therefore, in laser surface heat treatment by high-energy, most ferrite particles have been solved. In [Figure 15-b](#), there are two types of carbide particles, one in the form of Plate like carbides, in the grain boundary and another in the form of globular carbides that spread in the grain. In [Figure 15-d](#), in a laser-hardened samples of AISI 420, the Plate like carbides in the boundary are dissolved, but the globular carbides remain unchanged. So, laser energy leads to the dissolution of the chromium Plate like carbides in the grain boundary and globular carbides remain in the field of tempered martensite.

### 3-5 XRD Graphs of AISI 410 and AISI 420

XRD graphs of the base metal and laser hardened area for AISI 410 and AISI 420 are shown in Figure 16 and 17, respectively.

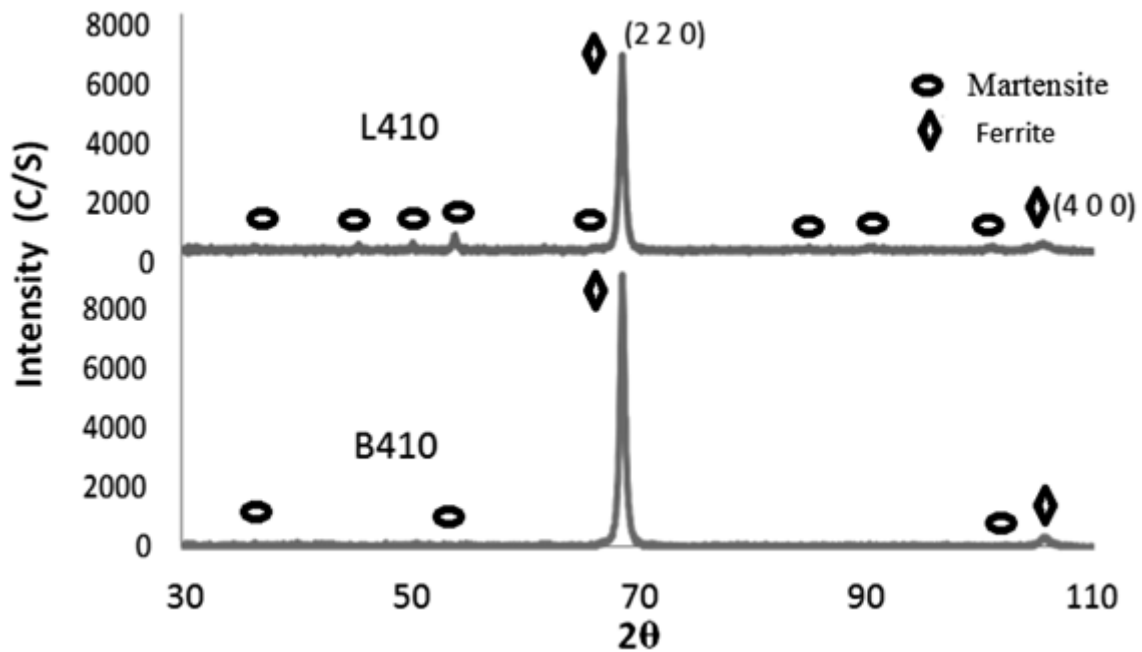


Fig.16 images of XRD graphs for the as-received (B410) and the laser hardened zone (L410)

By analyzing the XRD graphs of the AISI 410 and AISI 420 steels, the Martensite-Ferrite phases, and also the Martensite-Ferrite-Carbide phases, are observable respectively.

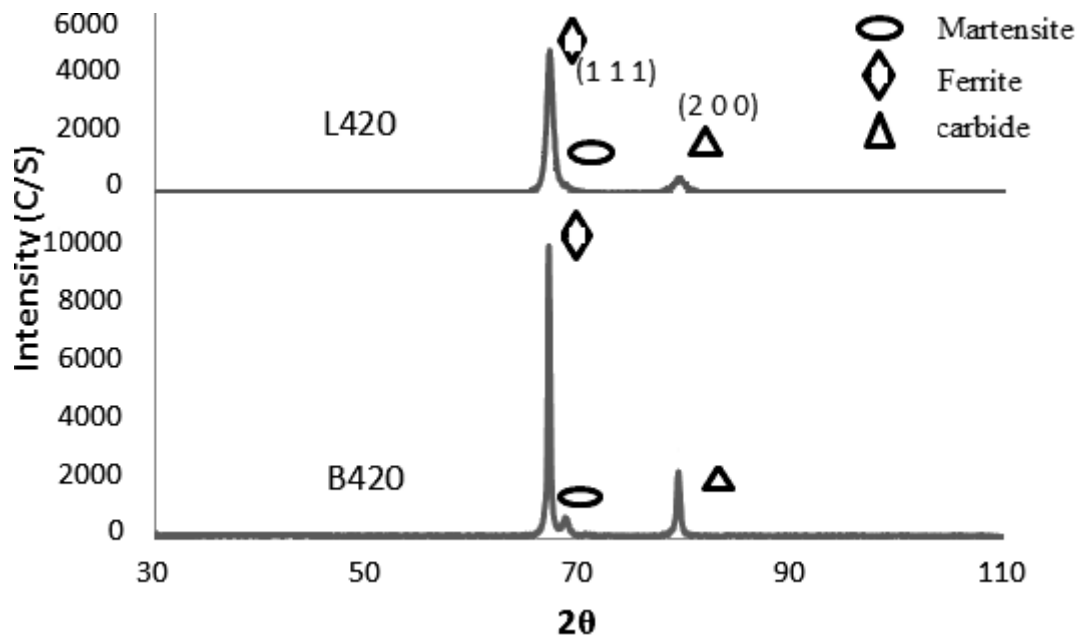
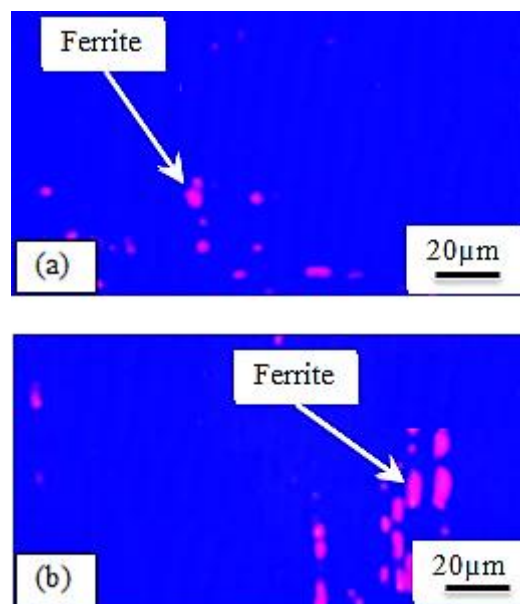


Fig. 17 images of XRD graphs for the as-received (B420) and the laser hardened zone (L420)

As can be seen, the XRD graphs confirm the presence of ferrite particles for AISI 410, ferrite and carbides particles for AISI 420 in martensite field. It is concluded from [Figures 16 and 17](#) that the ferrite, carbide and martensite phases in the hardened area of AISI 410 and AISI 420 is smaller than raw material and this size reduction in AISI 420 is higher than AISI 410.

### **3-6 Percentage of Ferrite Phase in AISI420 and AISI410**

After taking microstructure images with an optical microscope, the particle of the ferrite phase in the martensite field of the AISI 410 and AISI 420 by using Celemex software was investigated. Given that the ferrite is a soft phase and its presence in the structure reduces the hardness and the strength, it is therefore necessary to identify and evaluate its amount in the steel. [Figure 18](#) shows images taken from the Celemex software. The images show that ferrite particles in hardened samples of AISI 420 ([Figure18-a](#)) are finer than AISI 410 ([Figure18- b](#)). Ferrite particles are red in color and the martensitic background is blue. The values of ferrite percentages in hardened area of all samples are presented in [Table 2](#).



**Fig. 18** Images of ferrite phase in martensitic field for the hardened samples by using Celemex software **a)** AISI 420 **b)** AISI 410

[Figure 19](#) shows the comparison of ferrite particles in the hardened area of AISI 420 and AISI 410 stainless steels.

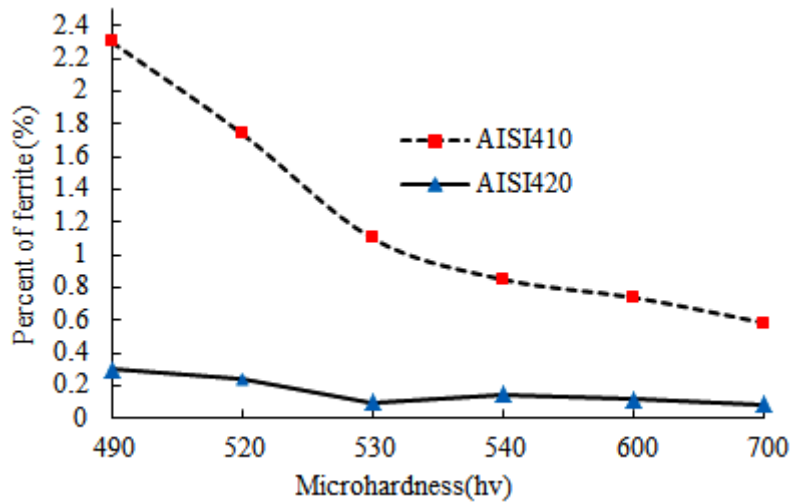


**Fig.19** Comparison of the ferrite phase of AISI 410 and AISI 420

It can be deduced from [Figure 19](#), with increasing hardness, the percentage of ferrite particles in the hardened area of AISI 420 and AISI 410 decreases, and this reduction in the AISI 420 is more than AISI 410. Because of the higher hardness and the smaller grain size of the austenitic in the AISI 420 than AISI 410, the ferrite particles dissolved in the grain and their size is smaller or disappears.

### **3-6 Furnace hardening heat treatment of AISI 410 and AISI 420**

According to the heat treatment cycle presented in section 2, [Figure 7](#), furnace heat treatment was conducted on both AISI 410 and AISI 420. The samples were quenched with 3 methods (air, oil, and water cooling). The hardness of quenched samples in the air, oil, and water for AISI 410 stainless steel were 412 Vickers, 434 Vickers, and 446 Vickers, while for AISI 420 were 513 Vickers, 528 Vickers, and 560 Vickers, respectively. [Table 5](#) illustrates the hardness of furnace hardening heat treatment and laser hardening of AISI 410 and AISI 420.

**Table.5** Comparison of hardness of furnace hardening heat treatment and laser hardening of AISI 410 and AISI 420.

| Cycle of heat treatment | Furnace hardening heat treatment of AISI 410 | Furnace hardening heat treatment of AISI 420 | Laser hardening of AISI 410 | Laser hardening of AISI 420 |
|-------------------------|--|--|-----------------------------|-----------------------------|
| Quenching in oil        | 434 (h v)                                    | 528 (h v)                                    | -                           | -                           |
| Quenching in water      | 446 (h v)                                    | 560 (h v)                                    | -                           | -                           |
| Quenching in air        | 412 (h v)                                    | 513 (h v)                                    | -                           | -                           |
| Self-quenching by laser | -  | -  | 620 (h v)                   | 720 (h v)                   |

By investigating the microstructure of the AISI 410 and AISI 420 after the furnace hardening heat treatment, cooling in the water environment have given a micro-crack, and in the air environment, the hardness has been reported to be the lowest value. So the oil environment has been evaluated as the ideal cooling environment for AISI 410 steel and AISI 420 steel at 434 Vickers and 528 Wacers hardness, respectively. as a result, the hardness of the diode laser hardening is 1.4 times the hardness of furnace hardening heat treatment of the AISI 410 and 2.5 times the hardness of furnace hardening heat treatment of the AISI 420.

In the furnace hardening heat treatment due to the holding the sample at 120 minutes in a temperature of 980 cantigrad degrees, as shown in [Figure 20-a](#), ferrite fine particles are distributed and dispersed in the martensitic field. However, these particles are interconnected and regular in the laser hardening process.

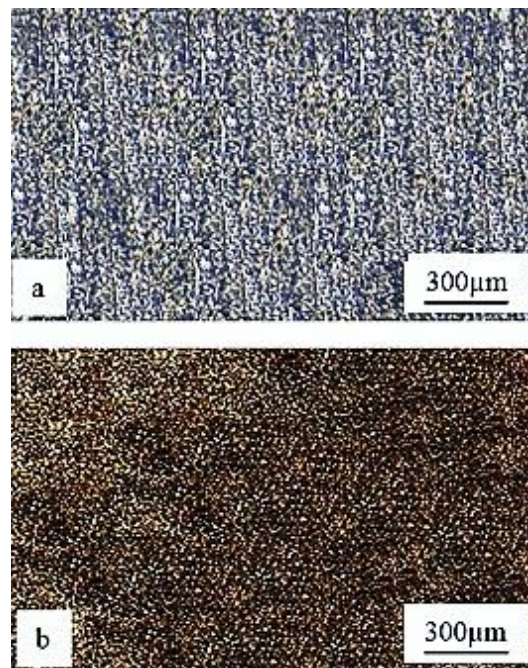


**Fig. 20** Images of Microstructure of furnace hardening heat treatment, AISI 410#**a** & AISI 420#**b**

In the laser hardening, due to the high energy concentration, localized hardness occurs, while in the furnace hardening heat treatment, hardness is volumetric. The presence of ferrite particles in the Martensite field reduces the hardness and strength of the steel. Due to short interaction time in the laser and high speed of the process, ferrite particles are observed in the Martensite field. In order to reduce or eliminate them, high laser power and the low scanning speed could overcome the problem. In furnace hardening heat treatment because of keeping the sample at a specific time during the heating cycle, the ferrite particles become finer or

maybe disappear. Therefore, in heat treatment cycle of furnace hardening the hardness increases due to the formation of a structure consisting of a uniform martensitic phase, but this structure is brittle. In laser hardening, by choosing the proper and appropriate input parameters, it is possible to obtain a better hardness and the more mechanical properties than the furnace hardening heat treatment. [Figures 20-a](#) and [20-b](#) shows that particles of ferrite and carbide in 410 and 420 samples of the furnace hardening heat treatment, are very tiny and scattered.

#### **4 - CONCLUSION**

In this paper, the effect of diode laser surface hardening of AISI 410 and AISI 420 stainless steel in order to compare the material behaviour was investigated with the same input parameters. According to the experiments, the following results are obtained from the present study:

1. Due to the higher carbon content, homogeneity of the structure and finer grain size of the AISI 420 than the AISI 410, the hardenability of AISI 420 stainless steel is higher than AISI 410 stainless steel. Therefore, with the same laser hardening process input parameters, the hardness of AISI 420 is more than AISI 410.
2. Due to the smaller grain size of the AISI 420 than the AISI 410, the mechanical properties of the AISI 420 will be higher than the AISI 410.
3. Due to the stretch of particles in the AISI 410 structure and the higher percentage of alloying elements, which increases the thermal conductivity, the absorption of laser energy in AISI 410 will increase. Therefore, With the same laser hardening process input parameters, the depth and width of hardness area of AISI 410 is more than AISI 420.
4. The maximum hardness value obtained in diode laser hardening of AISI 410 (620 Hv) is about 1.4 times the furnace hardening heat treatment (434 Hv), and for AISI 420, it is (720 Hv) about 2.5 times the furnace hardening heat treatment (528Hv).
5. Transformation of the laser hardening for AISI 410 provides a structure consisting of a ferrite phase in the martensite field which is a result of solid state transformation and for AISI 420 provides fine-ferrite and carbide particles in the martensite field because of dissolution or/and redistribution of ferrites and carbides
6. Ferrite and carbide particles in the microstructure obtained from laser hardening are continuously but in the furnace hardening heat treatment are finer and more dispersed.

7. By increasing the hardness by laser hardening technique, the grain sizes reduces, and the strength of the material or mechanical properties improve.

#### ACKNOWLEDGMENTS

Authors are grateful to Iran National Science Foundation (INSF) via grant No. 95828673.

#### REFERENCES

1. J C. Ion, *Laser processing of engineering materials* pp.15-16, 2005.
2. P.Molian, *Surface modification technologies-An engineering guide* TS Sudarshan NewYork : Marcel 18, pp.14-31, 1989.
3. A H. Faraji, M Moradi, M Goodarzi, P. Coluccid, C.Maletta. An investigation on capability of hybrid Nd:YAG laser-TIG welding technology for AA2198 Al-Li alloy, *Optics and Lasers in Engineering*, Vol. 96, pp. 1-6, 2017.
4. M. Moradi, M. Ghoreishi, A. Khorram. Process and Outcome Comparison between Laser, Tungsten Inert Gas (TIG) and Laser-TIG Hybrid Welding. *Journal of lasers in Engineering*, Vol. 38, Issue 1-3, 2017.
5. M. Moradi, N. Salimi, M. Ghoreishi, H Abdollahi, M Shamsborhan, Parameter dependencies in laser hybrid arc welding by design of experiments and by a mass balance, *Journal of Laser Applications* 26 (2), 02, 2004.
6. J. Sundqvist, A. F. H. Kaplan, J. Granström, and K.G. Sundin, Identifying residual stresses in laser welds by fatigue crack growth acceleration measurement, *Journal of Laser Applications* 27, 042002, 2015.
7. M. Moradi, M. Ghoreishi, M. Torkamany, J. Sabbaghzadeh, M. J. Hamed, An investigation on the effect of pulsed Nd: YAG laser welding parameters of stainless steel 1.4418, *Advanced Materials Research*, Vol. 383, No. 24, pp. 6247-6251, 2012.
8. A. khorram, A Jafari, M Moradi. Laser brazing of 321 and 410 stainless steels using BNi-2 nickel-based filler metal. *Modares Mechanical Engineering* Vol.17 (1), 129-135, 2017.
9. E.M. Anawa & A. G. Olabi, "Effects of Laser Welding Conditions on Toughness of Dissimilar Welded Components", *Applied Mechanics and Materials*, Vol. 5-6, pp. 375-380, 2006.
10. M. Moradi, M.M Fallah, S. Jamshidi Nasab. Experimental Study of Surface Hardening of AISI 420 Martensitic Stainless Steel Using High Power Diode Laser. *Transactions of the Indian Institute of Metals* 71Vol. 8, pp 2043–2050, 2018.
11. J.M.F. Vollertsen, K. Partes, 2005, State of the art of laser hardening and cladding, *Proceeding of The Third International WLT*, Vol. 209, pp. 1-7, 2012.
12. M. Bojinovic, N. Mole, B. stok, a computer simulation study of the effects of temperature change rate on austenite kinetics in laser hardening, *Surface & Coatings Technology*, Vol. 273, pp. 60–76, 2015.
13. A.R Hamad, J.H Abboud, F.M Shuaeib, K.Y Benyounis, Surface hardening of commercially pure titanium by laser nitriding: Response surface analysis, *Advances in engineering software*, 2010.

14. J. H. Abboud, K.Y. Benyounis, H. Julifkar, MSJ Hashmi, Material Response With High Power Laser in Surface Treatment of Ferrous Alloys, 2014.
15. M. Moradi, E. Golchin. Investigation on the effects of process parameters on laser percussion drilling using finite element methodology; statistical modelling and optimization. *Latin American Journal of Solids and Structures*, Vol. 14, No 03 pp 464 – 484, 2017.
16. M. Moradi, O. Mehrabi, T. Azdast, K. Y. Benyounis, Enhancement of low power CO<sub>2</sub> laser cutting process for injection molded polycarbonate, *Optics & Laser Technology*, Vol. 96C, No. 06, pp. 208–218, pp.421, 2017.
17. H.A Eltawahni, K.Y Benyounis, A.G Olabi, High Power CO<sub>2</sub> Laser Cutting for Advanced Materials – Review, Elsevier 2016.
18. M. safari, M. farzin, Experimental investigation of laser forming of a saddle shape with spiral irradiating scheme, *Optic and laser technology*, vol.66, pp146-150, 2015.
19. M. safari, M. farzin ,H. mostaan,A novel method for laser forming of two-step bending of a dome shaped part, *Iranian journal of materials forming*, Vol.4, issue2, pp1-14, 2017.
20. H. mostaan, M. shamanian, S. hasani, j.A.szpunar, Nd: YAG Laser Micro-Welding of Ultra-Thin FeCo-V Magnetic Alloy Optimization of Weld Strength, researchgate, 2017.
21. M. safari, H. mostaan, Experimental and numerical investigation of laser forming of cylindrical surfaces with arbitrary radius of curvature, *Alexandria engineering journal* vol.55, NO. 3, pp.1941-1949, 2016.
22. M. safari, Exprimental and numerical investigation of laser forming of a doubly curved saddle shapewith spiral irradiating schem, *journal of advanced manufacturing technology* vol. 9, NO. 2, 2015.
23. Lin Li, The advances and characteristics of high-power diode laser materials processing, *Optics and Lasers in Engineering* Vol. 34, pp 231-253, 2000.
24. R. Li, Y. Jin, Z. Li, & K. Qi,” A Comparative Study of High-Power Diode Laser and CO<sub>2</sub> Laser Surface Hardening of AISI 1045 Steel”, *Journal of Materials, Engineering and Performance*: Vol. 23(9), pp3085-3091, 2014.
25. A.G. Olabi, M.S.J. Hashmi, The microstructure and mechanical properties of low carbon steel welded components after the application of PWHTs. *Journal of Materials Processing Technology*, Vol. 56, NO. 1–4, Pages 88-97, January 1996.
26. A.G. Olabi & M.S.J. Hashmi, Effects of post-weld heat-treatment soaking temperature on the mechanical properties and residual stresses of a martensite stainless-steel welded component, *Journal of Materials Processing Technology*, vol. 38, pp. 387-398, 1993.
27. A.G. Olabi, M.s.J. Hashmi, Effects of the stress-relief conditions on a martensite stainless-steel welded component, *Journal of Materials Processing Technology*, vol. 300, (3):216-225, May 1998.
28. A.G. Olabi, R. Lostado-Lorza, K. Y. Benyounis, Review of Microstructures, Mechanical Properties, and Residual Stresses of Ferritic and Martensitic Stainless-Steel Welded Joints, , *In book: Comprehensive Materials Processing*, May 2014.
29. B. Mahmoudi, A. R. Sabour Aghdam, M. J. Torkamany, Controlled laser transformation hardening of martensitic stainless steel by pulsed Nd:YAG laser, *Journal of electronic science and technology*, Vol. 8, No. 1, pp. 87-90, 2010.
30. Cordovilla.F, Garc’ia-Beltra’n.A, Sancho.P, Dom’inguez.J, Ruiz de Lara.L & Oca~na. J. L., Numerical/experimental analysis of the laser surface hardening with overlapped tracks to

- design the configuration of the process for Cr-Mo steels, *Materials & Design*, Vol. 102, No. 15, pp. 225-237, 2016.
31. G. Telasang, J. Dutta Majumdar, G. Padmanabham, I. Manna, Structure–property correlation in laser surface treated AISI H13 tool steel for improved mechanical properties, *Materials Science & Engineering A* 599, pp. 255–267, 2014.
  32. F. Aline Goia. & M. Sergio Fernandes Lima, Surface Hardening of an AISI D6 Cold Work Steel Using a Fiber Laser”, *Journal of ASTM International*, Vol. 8, No. 2, 2010.
  33. Gh. Zirepour, R. Shojaa Razavi, Evaluation of Electrochemical Corrosion Effects of AISI 420 Steel After Laser Surface hardening, *Journal of Science and surface engineering*, Vol. 22, pp. 71-79, 2014.
  34. K.Y. Benyounis. F. Shuaeib, An Indepth Investigation of Gas Nitriding of Stainless Steel: New DOE Parametric Studies and Optimization. Engineering. Oxford: Elsevier; pp 1-12, 2016.
  35. M. Moradi, M. Karami Moghadam, J. Zarei, B. Ganji. The effects of laser pulse energy and focal point position on laser surface hardening of AISI 410 stainless steel. *Modares Mechanical Engineering*. Vol. 17, No 7, pp. 311-318, 2017.
  36. H. Chandler, Heat Treater’s Guide, Practices and procedures for nonferrous alloys, the materials information company, 1996.
  37. A. Bień, M. Szkodo, Surface treatment of C80U steel by long CO2 laser pulses, *Journal of Materials Processing Technology*, Vol 217, pp. 114–121, 2015.
  38. M. Moradi, H. Arabi, Increasing the Surface Hardness of 410 Martensitic Stainless Steel Using High Power Diode Laser, *Journal of Science and surface engineering*, (35) pp: 59-70. 2018.
  39. M. R. Jelokhani-Niaraki, N. B. Mostafa Arab, H. Naffakh-Moosavy & M. Ghoreishi, The systematic parameter optimization in the Nd:YAG laser beam welding of Inconel 625, *The International Journal of Advanced Manufacturing Technology*, Vol. 84, NO 9–12, pp. 2537–2546, June 2016.
  40. M. Moradi, H. Arabi, Experimental modeling of laser surface hardening process of AISI 410 by Response Surface Methodology, *Modares Mechanical Engineering*; 18(03): 79-188, 2018.
  41. R. Li, Y. Jin, Zh. Li, & K. Qi, A Comparative Study of High-Power Diode Laser and CO2 Laser Surface Hardening of AISI 1045 Steel, *JMEPEG*, Vol. 23, pp. 3085–3091, 2014.
  42. R.E. Smallman, Modern physical Metallurgy, Furth Edition, Great Britain, The university of Birmingham, 1990.
  43. Bong-bu Jung a , Hun-kee Lee b, Hyun-chul Park, Effect of grain size on the indentation hardness for polycrystalline materials by the modified strain gradient theory, *International Journal of Solids and Structures* Vol. 50, pp 2719–2724, 2013.
  44. Xiaoming Liu, Fuping Yuan, Yueguang Wei, Grain size effect on the hardness of nanocrystal measured by the nanosize indenter, *Applied Surface Science* Vol. 279, pp 159-166, 2013.
  45. G.E. Dieter Jr, Mechanical Metallurgy, McGraw-Hill, 1961.
  46. K. E. Thelning, Steel and Its Heat Treatment, Bofors Handbook, Butterworths, 1967.
  47. M.A. Grossman, & E.C. Bain, Principles of Heat Treatment, 5th Ed., ASM International, 1964.